LUMINESCENCE AND HOST LATTICE STRUCTURE OF CRYSTALLINE MICRO AND NANOPARTICLES CO-DOPED WITH LANTHANIDE IONS

Nadia Khaled Zurba [(1),(2)] and José Maria da Fonte Ferreira [(1)]

[(1)] Ceramic and Glass Engineering Department, Centre for Research in Ceramic and Composite Materials (CICECO), University of Aveiro, 3810-193, Portugal
[(2)] Department of Materials Engineering (DEMA), State University of Ponta Grossa, Brazil
E-mail: f2698@ua.pt (Zurba N.K.)

ABSTRACT

This article reports the investigation of crystalline micro and nanoparticles co-doped with lanthanide ions, aiming at correlate their host lattice structure and chemical composition to the luminescence features. For this purpose, five phosphors were characterized by X-ray diffraction (XRD), scanning electron microscopy coupled to energy dispersive X-ray (EDX) spectroscopy, and photoluminescence (PL) spectroscopy, namely performed by their chromatic coordinates, radiance, luminance and PL emission spectra. This type of investigation concerning the optical characterization of luminescent crystalline micro and nanoparticles doped with lanthanide ions might be useful for scientific and practical applications, such as in light-emitting devices, luminescent paintings, ceramics, sensors, in nanoscience and nanotechnology.

Key-words: Luminescence, Host Lattice, Nanocrystals, Nanoparticles, Lanthanide.

1. INTRODUCTION

A timely topic in nanomaterials and nanotechnology is the design, synthesis, and control of the optical properties of photoluminescent (PL) crystalline compounds[1]. To date, much work in this field has focused on the quantum dots (QDs) of narrow band gap semiconductors sulphides (e.g. ZnS, CdS)[2], silicon (Si QDs, porous Si)[3] and strontium aluminate nanomaterials[4,5]. The correlation between structures and photo-emission properties of luminescent particles constitutes a relevant subject for fundamental materials research.

The luminescence of micro and nanocrystals usually comes from the band gap and the various defects, which the band gap and defect emissions of phosphors might be located in the UV and visible (400–600 nm) regions[6]. The control of their optical features has deserved a progressive attention for long-afterglow applications, bioimaging, biosensors and photocatalysis. However, the persistent luminescence emission in phosphors might be also derived from powder mixtures, and the control remains difficult, albeit essential for the development of new photonic materials, photocatalysts, and devices.

More specifically, strontium aluminate co-doped with lanthanide ions[4] ($SrAl_2O_4$:Ln) is a type of luminescent material about 10 times brighter, 10 times longer glowing, and 10 times more expensive than its predecessor copper activated zinc sulphide[6] (ZnS:Cu). Strontium aluminate phosphors produce yellow-green, blue-green and blue hues, for the excitation wavelengths from 200 to 450 nm, with wavelength emission at ≈ 520 nm, blue-green at ≈ 505 nm, and blue at ≈ 490 nm, depending of the lanthanide co-doping. Note that "*phosphor*" is a term herein used to designate a lighting material, and does not refer to the chemical element P. This word '*phosphor´* was invented in the 17th century from a sintered stone that emitted red light in the dark after exposure to sunlight, called "*Bolognian stone*" (actually known as being BaS) in the pigment industry[6].

The luminescence characterization[6-8] of phosphors is usually performed with the following two types of spectra: excitation spectrum, giving the information on the positions of excited states that result in the emission of light; and emission spectrum that provides information on the spectral distribution of the light emitted by a sample produced from an excitation source. The optical characterization is also determined by the afterglow emission features, namely by the luminance that is the light reflected

by the surface in a given direction measured in candelas per square metre (cd/m^2), and radiance (μW/cm^2). Furthermore, since 1931 when the *Commission International de l'Éclairage* (CIE) created a standardized system of quantitative colour measurement[6], luminescence features might be also characterized by the colour appearance in chromatic coordinates.

In this article, we report on an experimental study of crystalline micro and nanoparticles co-doped with lanthanide ions, aiming at correlate their host lattice structure and chemical composition to the luminescence features. For this purpose, five phosphors were characterized by X-ray diffraction (XRD), scanning electron microscopy coupled to energy dispersive X-ray (EDX) spectroscopy, and photoluminescence (PL) spectroscopy, namely performed by their chromatic coordinates, radiance, luminance and PL emission spectra. This type of investigation concerning the optical characterization of luminescent crystalline micro and nanoparticles doped with lanthanide ions might be useful for scientific and practical applications, such as in light-emitting devices, luminescent paintings, ceramics, biosensors, in nanoscience and nanotechnology.

2. EXPERIMENTAL

Crystalline phosphor materials co-doped with lanthanide ions were investigated as-received (*c*ommercial powders, China). X-ray diffraction (XRD) was used to characterize the structure of the crystalline host lattices of samples. For this purpose, a high-resolution Rigaku Geigerflex D/Mac, C Series diffractometer was used with Cu $K\alpha$ radiation (λ = 1.5406 Å) produced at 30 kV and 25 mA scanned the diffraction angles (2θ) between 20º and 50º with a step size of 0.02º 2θ per second. The positions of the characteristic peaks were indexed to standard cards JCPDS Powder Diffraction Files (PDF) of the International Centre for Diffraction Data (ICDD).

Powder microstructure and elemental composition of samples were analysed via scanning electron microscopy (SEM) coupled to energy dispersive X-ray (EDX) spectrometer in a SU-70 microscope at University of Aveiro. SEM SU-70 conditions: accelerating voltage from 4 to 15 kV, magnification of 35,000 in working distance from 2 to 7 mm using an emission current of 32,000 nA. The EDX measurements were obtained in a Bruker AXS Microanalysis GmbH, Germany. The energy of the

beam was in the range of 10-20 keV Puls, 2.92 kcps, and caused X-rays emitted from the point the material.

Photoluminescence (PL) data were recorded at room temperature on a Fluorolog-3 Model FL3 – 2T with double excitation spectrometer and a single emission spectrometer using a monochromator (TRIAX 320) coupled to a Hamamatsu R928 photomultiplier, in a front face acquisition mode (Physics Department of University of Aveiro, Portugal). The excitation source was a Xenon lamp. Measurements of colour appearance from emission/excitation curves were carried out under the same conditions calibration to measure the intensity reliability. The selected wavelengths passed through a body (tube) filled with transparent water with known peak emission at 397 nm for calibration of the equipment by using the Datamax software.

3. RESULTS AND DISCUSSIONS

3.1. Crystalline host lattices

XRD patterns of micro and nanoparticles of oxides and sulphides co-doped with lanthanide (Ln) ions are shown in **Fig. 1.** These luminescent compounds have their colour appearance in the UV-VIS region, emitting around the yellow-green, red and orange.

The corresponding structures indicate that all of these compounds are crystalline, which host lattices where the luminescent centres (Ln= Eu, Dy, Ce, Tm) are located are formed of one or more type of phosphors. Crystalline $SrAl_2O_4$ host lattice was identified as the matrix of luminescent yellow-green phosphor (**Fig. 1**(a)), in agreement with previously reported in the literature[4,6]. Note that a mixture of Ca atoms in the crystals provides a lattice structure for $(Ca,Sr)Al_2O_4$ red phosphor, as depicted in **Fig. 1**(b). The red phosphor might be also obtained from calcium or strontium sulphide, i.e. (Ca,Sr)S, as demonstrated in **Fig. 1**(c). Interestingly, the secondary nature of the orange colour is well-evidenced by its obtaining through yellow + red phosphors, as comprised by [$SrAl_2O_4$ + $(Ca,Sr)Al_2O_4$] or [Y_2O_3 + CdS + PO_4] powder-mixtures, **Fig. 1**(d-e), respectively.

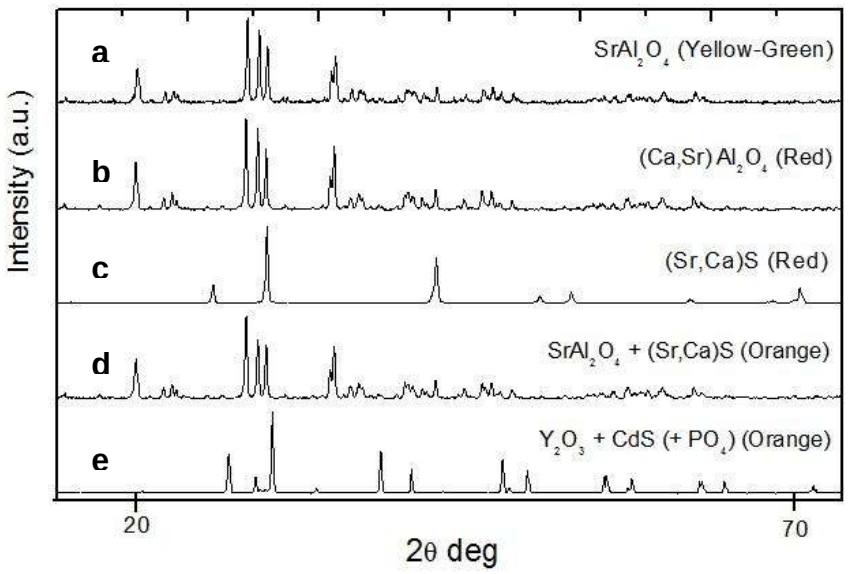

Figure 1. XRD patterns of the crystalline host lattices of luminescent micro and nanoparticles co-doped with lanthanide ions: a) $SrAl_2O_4$; b) $(Ca,Sr)Al_2O_4$; c) (Sr,Ca)S; d) $SrAl_2O_4$ + (Sr,Ca)S; and e) Y_2O_3 + CdS + PO_4.

2.2. SEM-EDX of micro and nanoparticles

SEM images of luminescent crystalline $SrAl_2O_4$ (**Fig. 2** (a-b)), $(Ca,Sr)Al_2O_4$ (**Fig. 2** (c-d)); Sr,Ca)S (**Fig. 2** (e-f)), $SrAl_2O_4$ + (Sr,Ca)S (**Fig. 2** (g-h)), and CdS + PO_4 (**Fig. 2** (i-j)) based materials indicate that they are composed of micro and nanoparticles and agglomerates from powder mixtures of different particle shapes and sizes. The corresponding semi-quantitative analyses of these luminescent phosphors, as observed in **Fig. 2,** are described in **Tab. 1**.

Note that Eu, Dy, Ce and Tm are the lanthanide elements commonly used as co-dopants of the host lattices[8]. Elements with high atomic number are easier to detect by EDX, as a convenient technique to analysis of lanthanide series (Z>58). Even doped with Eu^{+3} and Eu^{2+} ions, the PO_4 host lattice was also copper co-doped activating the PL red emission of PO_4:Eu, Cu phosphor, in agreement with other compounds reported elsewhere[6].

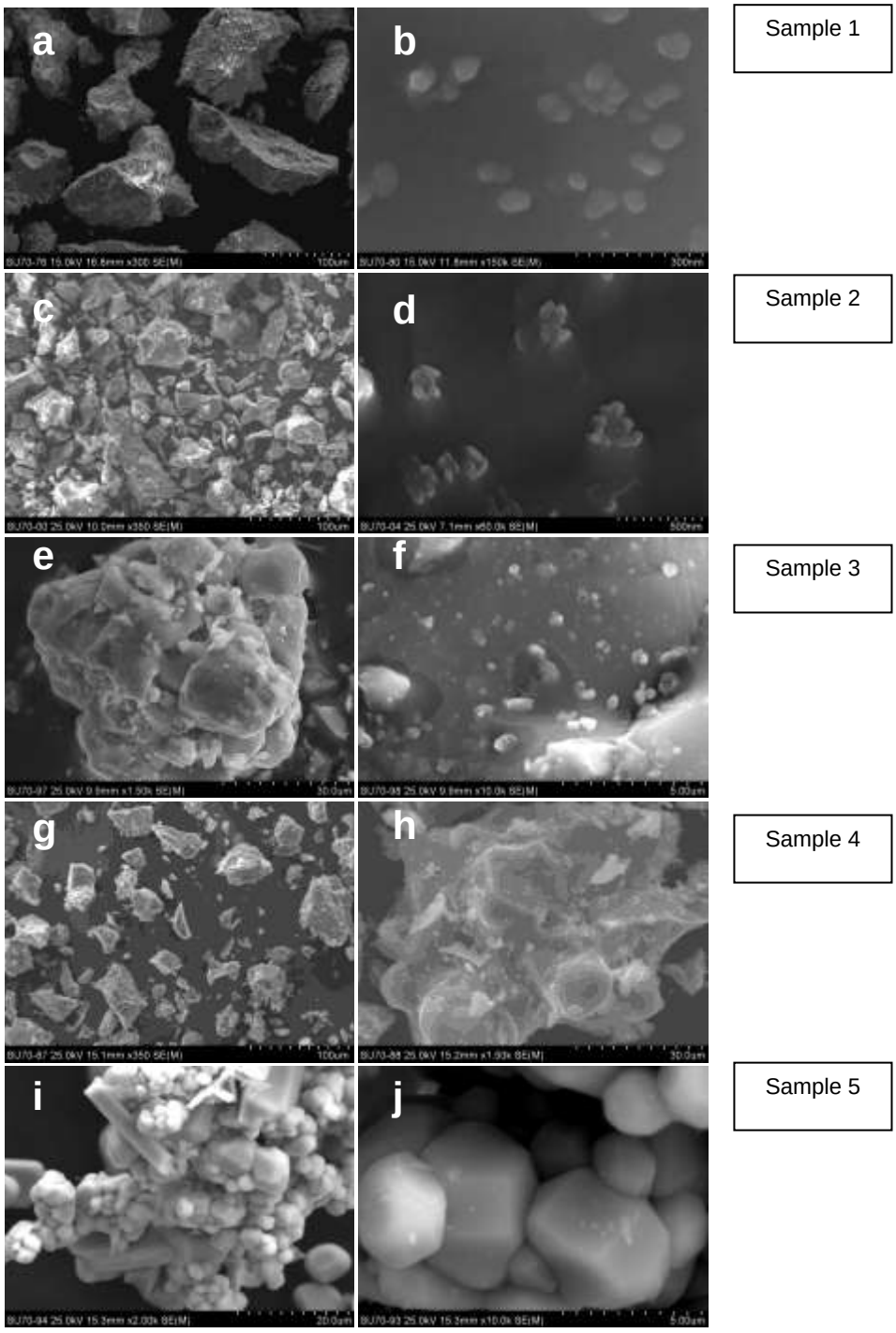

Figure 2. SEM observations of luminescent micro and nanoparticles: (a-b) $SrAl_2O_4$ (yellow-green); (c-d) $(Ca,Sr)Al_2O_4$ (red); (e-f) (Sr,Ca)S (red); (g-h) $SrAl_2O_4$ + (Sr,Ca)S (orange); and (i-j) Y_2O_3 + CdS + PO_4 (orange).

Table 1. Chemical composition of micro and nanoparticles co-doped with lanthanide ions by using a EDX Bruker AXS Microanalysis system, GmbH, Germany.

Sample	Element	series	[wt.-%]	norm. [wt.-%]	norm. [at.-%]	Error %
Yellow-Green: $SrAl_2O_4:Eu^{2+}, Dy^{3+}, Ce^{3+}$	Aluminium	K-series	14,83	10,43	11,14	1,61
	Strontium	K-series	64,49	45,37	14,93	1,91
	Europium	L-series	0,35	0,25	0,05	0,05
(sample 1)	Dysprosium	L-series	1,14	0,80	0,14	0,07
	Cerium	L-series	0,78	0,55	0,09	0,06
	Oxygen	K-series	54,86	38,59	69,53	6,63
		Sum:	142,14	100,00	100,00	
Red: (Ca,Sr) Al_2O_4:Ln	Aluminium	K-series	23,38067	18,43633	24,05746	1,23992
	Strontium	K-series	68,21949	53,79303	21,61547	1,996553
(sample 2)	Silicon	K-series	6,640471	5,236202	6,564116	0,333403
	Sulfur	K-series	0,101284	0,079865	0,087691	0,031664
	Europium	L-series	0,614945	0,484902	0,112345	0,04617
	Copper	K-series	0,598241	0,47173	0,261365	0,045921
	Calcium	K-series	0,006237	0,004918	0,004321	0,025997
	Oxygen	K-series	27,25712	21,49302	47,29723	3,641277
		Sum:	126,8185	100	100	
Red: (Sr, Ca)S	Sulfur	K-series	23,75004	16,42354	21,3955	0,888659
	Calcium	K-series	7,79269	5,388771	5,616737	0,25284
(sample 3)	Ytterbium	L-series	1,127446	0,779647	0,188214	0,0555
	Aluminium	K-series	0,822617	0,568853	0,880711	0,066118
	Strontium	K-series	81,25264	56,18751	26,7878	2,290472
	Silicon	K-series	11,31223	7,822587	11,63506	0,522435
	Oxygen	K-series	18,55212	12,82909	33,49598	2,240466
		Sum:	144,6098	100	100	
Orange: $SrAl_2O_4$ + (Sr,Ca)S	Aluminium	K-series	14,52131	10,13131	15,88487	2,542257
	Strontium	K-series	88,3634	61,64993	29,76554	2,69947
(sample 4)	Silicon	K-series	4,22815	2,949922	4,443374	0,25115
	Europium	L-series	2,776	1,936777	0,539164	0,120879
	Dysprosium	L-series	2,335263	1,629281	0,424157	0,117849
	Thulium	L-series	5,054821	3,526679	0,883147	0,180892
	Oxygen	K-series	26,05197	18,1761	48,05975	4,030885
		Sum:	143,3309	100	100	
Orange: Y_2O_3 + CdS + PO_4	Phosphorus	K-series	9,927659	9,927759	5,533295	0,41794
	Sulfur	K-series	0,867331	0,86734	0,466951	0,057924
(sample 5)	Aluminium	K-series	0,86493	0,864938	0,553407	0,096954
	Yttrium	L-series	2,825551	2,825579	1,736808	0,149535
	Curium	M-series	0,001	0,001	6,99E-05	0,025009
	Titanium	K-series	0,021049	0,021049	0,007589	0,026459
	Copper	K-series	0,506832	0,506837	0,137691	0,041292
	Europium	L-series	0,140305	0,140307	0,015939	0,031007
	Oxygen	K-series	84,84434	84,84519	91,54825	127,0824
		Sum:	99,999	100	100	

3.3. Optical characterization

In this section, the luminescence features of crystalline compounds are discussed by their chromatic coordinates, radiance and luminance (Section 3.3.1) and corresponding PL spectra (Section 3.3.2), as following described.

3.3.1. Chromatic coordinates, radiance and luminance

Luminescence data were recorded from three consecutive analyses by atomic excitations in discrete energy levels of the photons which passed through the monochromator aperture, as described in **Tab. 2**.

Table 2. Luminescence features of micro and nanoparticles lanthanide co-doped.

Colour Appearance	Atomic excitation [wavelength]	Chromatic coordinates		Integral			Radiance [$\mu W/cm^2$]	Luminance [cd/m^2]
		u	V	x	y	z		
a) Yellow-Green (sample 1)	$\lambda_{control}$ = 300 nm	0.1212	0.5466	0.2740	0.5492	0.1760	5,2849	22,6511
		0.1218	0.5455	0.2738	0.5450	0.1810	5,3565	22,6931
		0.1215	0.5461	0.2739	0.5474	0.1780	5,2540	22,4516
	$\lambda_{UV-lamp}$ = 360	0.1200	0.5483	0.2737	0.5557	0.1700	17,1	74,4864
		0.1199	0.5484	0.2735	0.5561	0.1700	17,1	74,1778
		0.1200	0.5484	0.2737	0.5560	0.1700	16,90	73,2735
	$\lambda_{max(1)}$ = 320 nm	0.1207	0.5480	0.2746	0.5541	0.1710	9,5664	41,3613
		0.1205	0.5482	0.2743	0.5548	0.1700	9,3403	40,5954
		0.1206	0.5484	0,2748	0.5555	0.1690	9,2949	40,4255
b) Red (sample 2)	$\lambda_{control}$ = 300 nm	0.4427	0.5316	0.6478	0.3457	0.0060	12,2	24,1642
		0.4429	0.5318	0.6484	0.3460	0.0050	12,1	23,9985
		0.4429	0.5316	0.6480	0.3457	0.0060	12,1	23,9935
	$\lambda_{UV-lamp}$ = 360	0.4441	0.5274	0.6419	0.3388	0.0190	5,757	10,6254
		0.4457	0.5280	0.6442	0.3392	0.0160	5,7493	10,6104
		0.4461	0.5283	0.6451	0.3396	0.0150	5,734	10,5905
	$\lambda_{max(1)}$ = 460 nm	0.4467	0.5329	0.6532	0.3463	0.0000	23,0	45,5964
		0.4460	0.5330	0.6528	0.3468	0.0000	23,0	45,5723
		0.4465	0.5329	0.6532	0.3464	0.0000	23,0	45,8506
c) Red (sample 3)	$\lambda_{control}$ = 300 nm	0.2777	0.5362	0.4913	0.4216	0.0870	15,6	48,76
		0.2759	0.5366	0.4898	0.4234	0.0860	15,3	47,934
		0.2747	0.5365	0.4881	0.4237	0.0880	15,3	47,9552
	$\lambda_{UV-lamp}$ = 360	0.2614	0.5369	0.4726	0.4314	0.0960	20,8	66,2726
		0.2617	0.5370	0.4732	0.4315	0.0950	20,8	66,1899
		0.2620	0.5370	0.4736	0.4314	0.0950	20,9	66,5837
	$\lambda_{max(1)}$ = 325 nm	0.2544	0.5376	0.4649	0.4366	0.0980	19,9	64,2873
		0.2543	0.5375	0.4647	0.4365	0.0980	20,2	65,0336
		0.2542	0.5375	0.4644	0.4365	0.0990	20,0	64,5872
	$\lambda_{max(2)}$ = 460 nm	0.4242	0.5348	0.6375	0.3572	0.0050	20,8	51,6129
		0.4273	0.5344	0.6396	0.3555	0.0040	20,9	50,9838
		0.4251	0.5349	0.6385	0.3570	0.0040	21,0	51,635
d) Orange (sample 4)	$\lambda_{control}$ = 300 nm	0.2965	0.5445	0.5266	0.4299	0.0430	32,0	116,2720
		0.2961	0.5445	0.5261	0.4300	0.0430	31,8	115,6465
		0.2960	0.5445	0.5260	0.4301	0.0430	31,9	115,7402
	$\lambda_{UV-lamp}$ = 360	0.2743	0.5452	0.5014	0.4429	0.0550	33,8	124,2767
		0.2744	0.5451	0.5014	0.4428	0.0550	33,9	124,5278
		0.2742	0.5451	0.5012	0.4429	0.0550	33,8	124,3036
	$\lambda_{max(1)}$ = 350 nm	0.2725	0.5450	0.4990	0.4436	0.0570	33,6	124,0512
		0.2726	0.5450	0.4991	0.4435	0.0570	33,8	124,7798
		0.2724	0.5451	0.4990	0.4437	0.0570	33,6	124,0414
	$\lambda_{max(2)}$ = 450 nm	0.3704	0.5437	0.6035	0.3937	0.0020	39,1	138,2148
		0.3706	0.5436	0.6035	0.3935	0.0030	40,0	136,2097
		0.3705	0.5436	0.6035	0.3936	0.0020	41,0	139,4847
	$\lambda_{max(3)}$= 530 nm	0.3818	0.5426	0.6126	0.3869	0.0000	33,1	110,4565
		0.3815	0.5426	0.6124	0.3871	0.0000	32,9	110,1012
		0.3816	0.5426	0.6124	0.3870	0.0000	33,7	112,7047
e) Orange (sample 5)	$\lambda_{control}$= 300 nm	0.2895	0.5328	0.4999	0.4089	0.0910	5,3253	16,8772
		0.2894	0.5335	0.5008	0.4103	0.0880	5,2559	16,7538
		0.2890	0.5331	0.4999	0.4098	0.0900	5,2762	16,8348
	$\lambda_{UV-lamp}$ = 360	0.3020	0.5376	0.5217	0.4127	0.0650	9,093	28,41
		0.3026	0.5379	0.5228	0.4131	0.0640	9,6873	30,1011
		0.3026	0.5384	0.5237	0.4142	0.0620	9,6455	30,0593
	λ_{max} = 340 nm	0.2933	0.5370	0.5109	0.4157	0.0730	13,9	44,5942
		0.2927	0.5368	0.5098	0.4155	0.0740	14,0	45,0085
		0.2926	0.5367	0.5095	0.4153	0.0750	14,0	44,8179

The spectral intensities, as a number of photons that passed through the slits, were selected at different wavelengths having sufficient energy to irradiate the excited samples: firstly, upon atomic excitation at 300 nm ($\lambda_{control}$), secondly, at 360 nm ($\lambda_{UV-lamp}$), which values were increased with sufficient energy up to detect the maximum excitation wavelength (λ_{max}) for each sample.

$SrAl_2O_4$ was clearly identified as the most bright luminescent material, since its radiance and luminance were performed with the highest values, both in the yellow-green (sample 1 - $SrAl_2O_4$: Eu^{2+}, Dy^{3+}, Ce^{3+}) phosphor or in the orange (sample 4 - $SrAl_2O_4$ + (Ca,Sr)S):Dy, Tm) powder-mixture phosphor. For instance, note that the presence of some impurities is also an efficient technique to improve the luminescence features in terms of colour appearance and luminance.

3.3.2. Photoluminescence emission spectra

Fig. 3 describes the photoluminescence emission spectra of the crystalline compounds which presence of Eu, Dy, Ce or Tm lanthanide ions was identified, in agreement with chemical identification performed by SEM-EDX (**Tab. 1**). In $SrAl_2O_4$ yellow-green sample (1), it was observed a large band with highest luminescence emission peaking at 525 nm[5], coherent with the atomic excitations depicted in **Tab. 2**(a) and luminescence centres present on its structure[9-11].

Note that in the graphics of **Fig. 3,** all samples (1), (2), (3), (4) or (5) revealed equal emission peaks (a)-(c), which luminescence data represent that the photoluminescence effect is mainly due to the same luminophor elements emitting the photons. Analysis of samples (2) and (5) was performed with the initial emission 300 nm, and identified the existence of two emission peaks which were measured separately, as excitations depicted in **Tab. 2** (b) and (e), respectively.

The predominance of thin emission peaks in the red sample (3), **Fig. 3**, clearly evidences the occurrence of (intra) f-f and (inter) f-d configurational transitions of the lanthanide ions[8], namely by Eu^{2+} and Eu^{3+} shifts in the red spectral region. In the orange sample (5), occurs an overlap of excitation peaks, certainly for the presence of more than one phosphor component.

Analysis of the orange sample (5) showed the peaks which reflect the heterogeneous impurity of a tertiary colour, so photoluminescence emission at different wavelengths – XRD patterns from **Fig. 1** proved that it is resulted from the mixture of different oxides/compounds, in contrast to the sample (4) which orange emission is derived by a combination of the yellow-green host lattice with the a significant amount of lanthanide co-dopants having emission shifts in the red region, such as Eu, Dy and Tm ions.

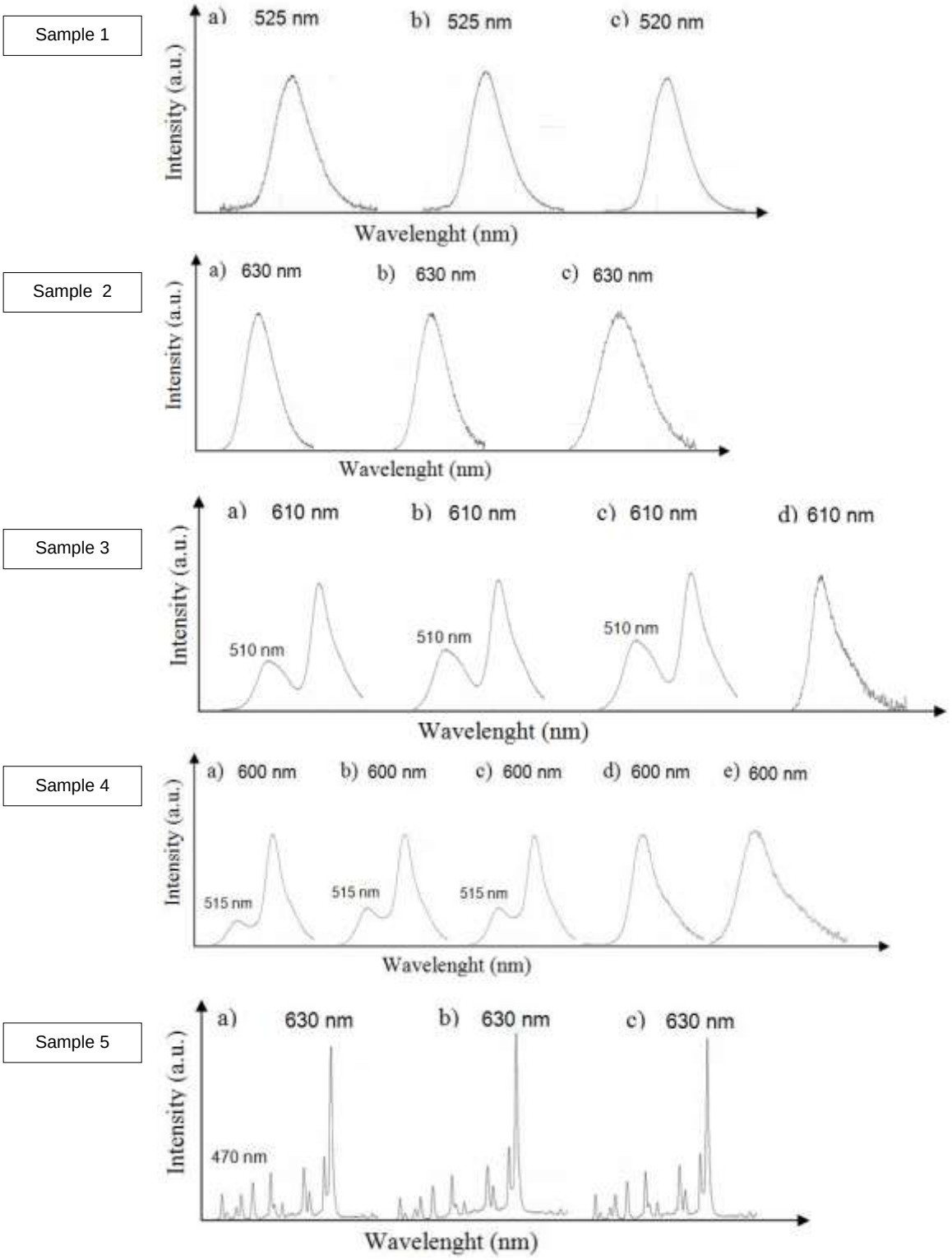

Figure 3. PL emission spectra of crystalline micro and nanoparticles, which curves were obtained under different excitations at (a) 300 nm (control), (b) 360 nm (UV-lamp), or at maximum wavelengths (c-d).

4. CONCLUSIONS

Luminescent micro and nanoparticles were characterized by XRD, SEM-EDX, and PL spectroscopy. Combining the versatile emission shifts of lanthanide ions as co-dopants that have electronic intra- and inter- configurational transitions with their host lattice structure, luminescent phosphors are produced. Their persistent luminescence features might be particularly important in nanotechnology and a promising candidate for new photoelectron devices, sensors, and long afterglow-in-the-dark applications. This research provides a practical strategy to obtain and characterize phosphorescent nanomaterials for a wide range of applications in luminescence.

REFERENCES

[1]. BRUCHEZ JR., M; MORONNE, M; GIN, P; WEISS, S; ALIVISATOS, A. P. Semiconductor Nanocrystals as Fluorescent Biological Labels. Science, 281, 2013-2016 **(1998)**

[2]. a) GREEN M. Angew. Chem. Int. Ed., 43, 4129 **(2004)**; b) GILL, R; ZAYATS, M; WILLNER, I. Angew. Chem. Int. Ed., 47, 7602 **(2008)**; c) STRANDWITZ, N.C; KHAN, A; BOETTCHER S.W; MIKHAILOVSKY, A.A; HAWKER, C.J; NGUYEN, T.Q; STUCKY, G.D. J. Am. Chem. Soc., 130, 8280 **(2008)**

[3]. a) KANG, Z.H; TSANG, C.H.A; WONG, N.B; ZHANG, Z.D; LEE, S.T. J. Am. Chem. Soc., 129, 12090 **(2007)**; b) WARNER, J.H; HOSHINO, A.; YAMAMOTO, K; TILLEY, R.D. Angew. Chem., Int. Ed., 44, 4550 **(2005)**; c) PARK, J.H; GU, L; GEOFFREY, M; RUOSLAHTI, E; BHATIA, S.N; SAILOR, M.J. Nat. Mater., 8, 331 **(2009)**

[4]. a) ZURBA, N. K; BDIKIN, I; KHOLKIN, A; GOLBERG, D; FERREIRA, J.M.F. Intercrystalline distal-effect on the afterglow phenomenon in photoluminescent $SrAl_2O_4:Eu^{2+}$, Dy3+, Ce^{3+} nanotube growth. Nanotechn., 21, 32, 325707 **(2010)** DOI:10.1088/0957-4484/21/32/325707; b) ZURBA, N.K. Luminescent beryllium, magnesium, calcium, strontium and barium aluminate nanotubes doped with cerium (III) and co-doped with other lanthanide ions, $M_{(1-x-y)}N_2O_4:Ce_x$, Ln_y, PCT Patent

104,486 **(2009)**; c) CHENG, B; LIU, H; FANG, M; XIAO, Y; LEI, S; ZHANG, L. Chem. Commun., 8, 944 **(2009)**; d) YE, C; BANDO, Y; SHEN, G; GOLBERG, D. Angew. Chem., 118, 5044 **(2006)**; e) YE, C; BANDO, Y; SHEN, G; GOLBERG, D. Angew. Chem. Int. Ed., 45, 4386 **(2006)**; f) AITASALO, T; HOLSA, J; JUNGNERD, H; JUNGNER, H**;** LASTUSAARI, M; NIITTYKOSKI, J**.** J. Lumin. 94, 59 **(2001);** g) LIN, Y.H; ZHANG, Z.T; ZHANG, F; TANG, Z.L; CHEN, Q.Y. Preparation of the ultrafine $SrAl_2O_4$:Eu, Dy needle-like phosphor and its optical properties, Mater. Chem. Phys., 65, 103 **(2000)**; h) MATSUZAWA, T; AOKI, Y; TAKEUCHI, N; MURAYAMA, Y. A new long phosphorescent phosphor with high brightness $SrAl_2O_4:Eu^{2+}$, Dy^{3+}. J. Electrochem. Soc., 143, 2670–2673 **(1996)**

[5]. ZURBA, N.K. Persistent luminescence of $SrAl_2O_4$:Ce(III), Dy, Eu nanotubes, nanowires and core-shells for people with disabilities: nano-emergency **(2010)** 168p. Thesis (PhD in Materials Science and Engineering) Centre for Research in Ceramic and Composite Materials, CICECO - University of Aveiro, Portugal.

[6]. SHIONOYA, S; YEN, W.M. Phosphor Handbook. CRC Press **(1998)**

[7]. GRIBKOVSKII, V.P. Academy of Sciences of Belarus, Minsk, Luminescence of Solids. D. R.VIJ (Editor), Plenum Press **(1998)**

[8]. ASPINALL, H.C. Chemistry of the f-block elements. Netherlands: Overseas Publishers Association **(2001)** ISBN 90-5699-333-X.

[9]. a) AITASALO, T; DEREN, P; HOLSA, J; JUNGNER, H; KRUPA, J.C; LASTUSAARI, M; LEGENDZIEWICZ, J; NIITTYKOSKI, J; STREK, W. Persistent luminescence phenomena in materials doped with rare earth ions. J. Solid-state Chem., 171, 114–122 **(2003)**; b) HOLSA, J; JUNGNER, H; LASTUSAARI, M; NIITTYKOSKI, J. Persistent luminescence of Eu^{2+} doped alkaline earth aluminates $MAl_2O_4:Eu^{2+}$. J. Alloys Comp., 354, 326–330 **(2003)**

[10]. SHI, W.S; YAMADA, H; NISHIKUBO, K; KUSABA, H; XU, C.N. Novel structural behavior of strontium aluminate doped with europium. J. Electrochem. Soc., 151, 5, H97-100 **(2004)**

[11]. FU, Z; ZHOU, S; ZHANG, S. Study on optical properties of rare-earth ions in nanocrystalline monoclinic $SrAl_2O_4$:Ln (Ln= Ce^{3+}, Pr3+, Tb^{3+}). J. Phys. Chem. B, 109, 14396–14400 **(2005)**